

Hydrogen Cyanide in Nitrogen-Rich Atmospheres of Rocky Exoplanets

P. B. Rimmer^a, S. Rugheimer^{b,c}

^a*University of Cambridge Department of Earth Sciences, Downing St, Cambridge CB2 3EQ and University of Cambridge, Cavendish Astrophysics, JJ Thomson Ave, Cambridge CB3 0HE and MRC Laboratory of Molecular Biology, Francis Crick Ave, Cambridge CB2 0QH*

^b*Centre for Exoplanet Science, University of St. Andrews, School of Earth and Environmental Sciences, Irvine Building, North Street, St. Andrews, KY16 9AL, UK*

^c*University Oxford, Atmospheric, Oceanic, and Planetary Physics Department, Clarendon Laboratory, Sherrington Road, Oxford, OX1 3PU*

Abstract

Hydrogen cyanide (HCN) is a key feedstock molecule for the production of life's building blocks. The formation of HCN in an N₂-rich atmospheres requires first that the triple bond between N≡N be severed, and then that the atomic nitrogen find a carbon atom. These two tasks can be accomplished via photochemistry, lightning, impacts, or volcanism. The key requirements for producing appreciable amounts of HCN are the free availability of N₂ and a local carbon to oxygen ratio of C/O ≥ 1. We discuss the chemical mechanisms by which HCN can be formed and destroyed on rocky exoplanets with Earth-like N₂ content and surface water inventories, varying the oxidation state of the dominant carbon-containing atmospheric species. HCN is most readily produced in an atmosphere rich in methane (CH₄) or acetylene (C₂H₂), but can also be produced in significant amounts (> 1 ppm) within CO-dominated atmospheres. Methane is not necessary for the production of HCN. We show how destruction of HCN in a CO₂-rich atmosphere depends critically on the poorly-constrained energetic barrier for the reaction of HCN with atomic oxygen. We discuss the implications of our results for detecting photochemically produced HCN, for concentrating HCN on the planet's surface, and its importance for prebiotic chemistry.

1. Introduction

Hydrogen cyanide (HCN) is a key molecule for prebiotic photochemistry. HCN is a precursor molecule to amino acids via Strecker synthesis, where HCN is reacted with ammonia and an aldehyde to form various amino acids (Strecker, 1854), and has for this reason been invoked as the mechanism for generating the amino acid glycine in the Miller-Urey experiment (Miller, 1957). The structure of the nucleobase adenine (C₅H₅N₅) is effectively five connected HCN molecules. Adenine can be formed by

Email addresses: pbr27@cam.ac.uk (P. B. Rimmer), srm26@st-andrews.ac.uk (S. Rugheimer)

HCN reacting with its conjugate base and polymerizing, followed by photochemical rearrangement of the resulting HCN tetramer and further HCN polymerization (Ferris and Orgel, 1966; Sanchez et al., 1966, 1967; Sanchez and Orgel, 1970).

More recently, HCN has been discovered to be present at each of the initial photochemical reactions that produce lipids, amino acids and nucleosides, the three building blocks of life (Ritson and Sutherland, 2012; Patel et al., 2015; Xu et al., 2018). In this scenario, UV light is absorbed by hydrogen cyanide and hydrogen sulfide or bisulfite in water. The UV photon initiates photodetachment of an electron from the hydrogen sulfide or bisulfite, and the solvated electron reduces the hydrogen cyanide, forming an imine complex that, when hydrolysed, forms formaldehyde. This photochemical homology can continue, with the dissociated products of cyanide reacting with the product sugars.

Other plausible feedstock molecules generated from reactions involving HCN, such as cyanamide and cyanoacetylene, react with the sugars to form the pyrimidine nucleotides. In addition, these feedstock molecules, along with methylamine and nitrogen oxides, act as activating agents to facilitate the ligation of these building blocks into polypeptides, a key next step in prebiotic chemistry (Mariani et al., 2018).

HCN can be produced photochemically (Zahnle, 1986; Tian et al., 2011), by interaction of the atmospheric gas with energetic particles (Airapetian et al., 2016), by lightning (Chameides and Walker, 1981; Ardaseva et al., 2017), and by meteor impacts (Ferus et al., 2017). In each of these scenarios, the authors have recognized that reduced carbon-bearing species greatly facilitate the production of hydrogen cyanide. In some circumstances, especially with impacts, up to 1% of the affected gas can be converted into HCN, but again only with a relatively reduced gas, and in the presence of significant concentrations of molecular nitrogen or ammonia. The same events occurring in a gas of different composition, however, can result in trace amounts of HCN, less than 1 ppb.

Exoplanets can be seen as diverse laboratories for atmospheric and prebiotic chemistry, and so we need not be bound by constraints from early Earth atmosphere. Bulk atmospheric composition is given for rocky planet atmospheres under a wide variety of elemental abundance ratios (Hu and Seager, 2014). In addition, changes in the water inventory (Gao et al., 2015), the amount of hydrogen retained in the atmosphere (Pierrehumbert and Gaidos, 2011), and the concentration of molecular nitrogen (Wordsworth and Pierrehumbert, 2014), can have profound effects on the evolution of the planet's atmosphere. Here we will focus on more Earth-like planets, in terms of their nitrogen content and water inventories. Given the presence of molecular nitrogen as a dominant atmospheric constituent, the bulk atmospheric composition will here be represented largely in terms of the C/O ratio (see Fig. 1).

We present our methods for calculating the climate and photochemistry in Section 2, and then discuss the connection between the C/O ratio, the relative UV flux and HCN in Section 3. In Section 4 present the concentrations of HCN as a function of the C/O ratio, UV flux, and the barrier to destruction by atomic oxygen. We conclude with a discussion of these results (Section 5).

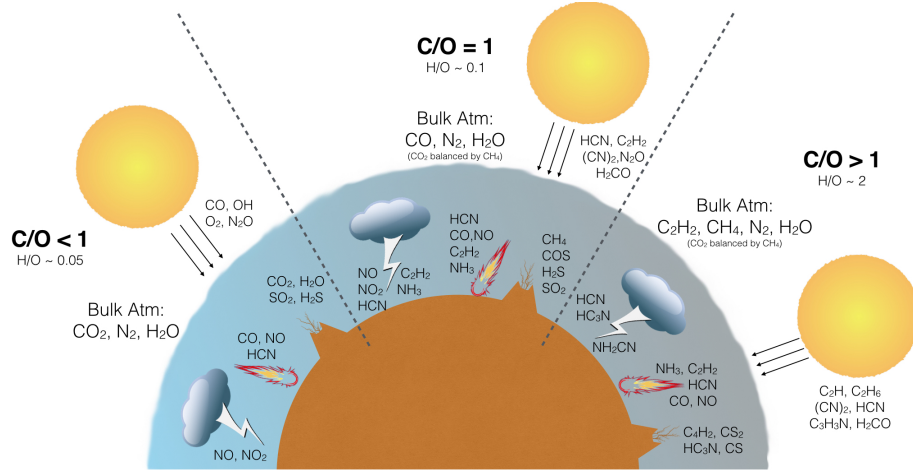


Figure 1: A representation of how the bulk chemistry changes with the bulk C/O ratio, and how more-or-less local chemical processes: lightning, impacts, volcanism, ultraviolet photons, are affected by the C/O ratio, from $C/O < 1$ to $C/O > 1$.

2. Methods

To calculate the temperature and pressure profiles, we use a 1D climate model developed for high- CO_2 /high- CH_4 terrestrial atmospheres (Pavlov et al., 2000; Kharecha et al., 2005; Haqq-Misra et al., 2008). This model simulates an anoxic 1 bar atmosphere composed of 89% N_2 , 10% CO_2 and 1% CH_4 , similar to some of the models of Zahnle (1986). Gases apart from H_2O are assumed to be well mixed in the atmosphere. The atmosphere was divided into 101 layers. The code uses a δ two-stream scattering approximation for the absorption of solar radiation (Toon et al., 1989) and 4-term, correlated k -coefficients to parameterize the absorption by the main greenhouse gases, namely: H_2O , CH_4 , and CO_2 . We use the solar evolution model for the incoming stellar radiation at 3.9 Ga (Claire et al., 2012), both for the climate modelling and the UV spectrum for the photochemistry discussed below. The temperature profile from the 1D climate model is in Fig. 2.

We take the prescribed stellar spectra and surface mixing ratios, and the temperature profile determined by the climate model, and apply them to the ARGO photochemistry/diffusion model (Rimmer and Helling, 2016), which solves the set of photochemical kinetics equations for a moving parcel of atmospheric gas:

$$\frac{\partial n_i}{\partial t} = P_i - L_i - \frac{\partial \Phi_i}{\partial z}, \quad (1)$$

Here, n_i [cm^{-3}] is the number density of species i , where $i = 1, \dots, I_s$, I_s being the total number of species. The quantity Φ_i is the flux of the species i into and out of the parcel when it is at height z . The parcel is used to give a chemical profile of the atmosphere, and UV photo-transport is calculated in order to determine the efficiency of the photochemistry at each parcel height (Rimmer and Helling, 2016). P_i [$\text{cm}^{-3} \text{ s}^{-1}$] and L_i

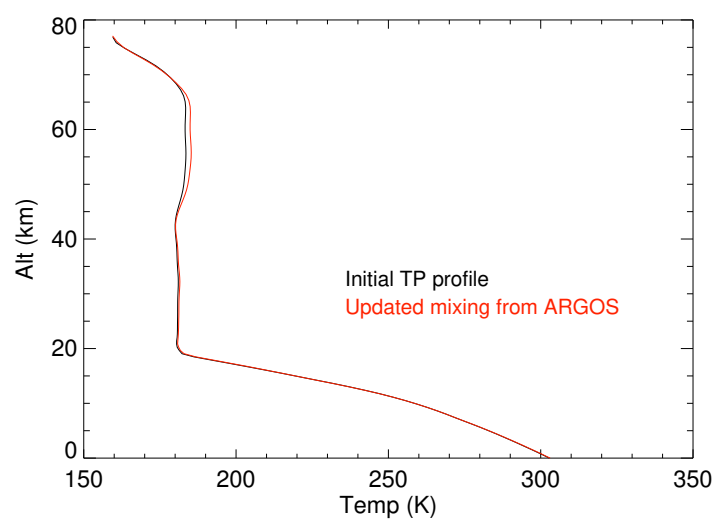


Figure 2: The temperature [K] as a function of altitude [km] for an anoxic 1 bar surface pressure atmosphere composed of 89% N_2 , 10% CO_2 and 1% CH_4 (black line), and with updated mixing ratios taken from the ARGOS photochemical model using the STAND2019 chemical network (red line).

[$\text{cm}^{-3} \text{ s}^{-1}$] represent the production and loss rates, which are determined by using the a modified version of the STAND2016 chemical network (Rimmer and Helling, 2016), which we hereafter will refer to as STAND2019. The network is described in detail below. This model will determine a different chemical profile from the climate model, but does not update the temperature profile. The deviation between the temperature profile for the initial and updated mixing ratios is small, and is shown in Fig. 2.

The STAND2019 chemical network is a modification of the STAND2016 network, which includes a robust H/C/N/O chemistry with species of up to 3 carbons, 2 nitrogens, 3 oxygens, and 8 hydrogens, valid for temperatures up to 30000 K, and including some relevant gas-phase reactions involving Na, K, Mg, Fe, Ti, Si, and Cl. Altogether, the STAND2019 chemical network comprises over 5000 reactions involving over 350 chemical species. The full network is included in the Supplementary Information. We now describe the most significant differences between STAND2016 and STAND2019. The reverse of a reaction relevant for formaldehyde in STAND2016 has been suppressed in the STAND2019 network in order to properly reproduce the formaldehyde (HCHO) abundances observed in Earth’s atmosphere today (Granville-Willett et al., 2018). The relevant reaction is:



and its reverse is:



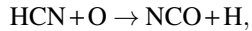
The reverse rate is calculated using the Gibbs free energy, as described by Rimmer and Helling (2016). This is so that the chemical steady state converges to thermochemical equilibrium at sufficiently long timescales in the absence of irreversible reactions (e.g. photochemistry). This is important for reproducing hot exoplanet atmospheric compositions and the gas-phase component of magma chemistries, both applications for the STAND2019 network. The consequence of this approach is that sometimes the barrier calculated by reversing the reaction does not reproduce the actual chemical barrier to the reaction, and in the case of R3, the barrier is greatly underestimated. In order to compensate for this, the rate constant for R3 is set to:

$$k = 6.0 \times 10^{-11} e^{-5370 \text{ K}/T} \text{ cm}^3 \text{ s}^{-1},$$

and using this rate constant, with this sizable barrier, reproduces the the formaldehyde (HCHO) abundances (Granville-Willett et al., 2018).

The forward and reverse barriers for this reaction will need to be revisited in the future to figure out why the barrier for R3 is considerably higher than determined when reversing R2.

In addition, the relevant reaction from STAND2016 has been replaced with R7:



with the rate constant of:

$$k = 1.43 \times 10^{-12} \left(\frac{T}{300 \text{ K}} \right)^{1.47} e^{-3770 \text{ K}/T} \text{ cm}^3 \text{ s}^{-1}, \quad (4)$$

from Perry and Melius (1985). This choice of rate constant will be justified in Section 4.2. Finally, we have added the reaction (Becker and Hong, 1983):



for which we assign a rate constant of:

$$k = 2.2 \times 10^{-12} \text{ cm}^3 \text{ s}^{-1}. \quad (6)$$

This reaction was added to see if cyanoacetylene might be generated in trace but significant quantities in our models, which would be relevant for prebiotic chemistry, as acyanoacetylene is one of the key feedstock molecules for forming some of the canonical amino acids and the pyrimidine nucleotides. It turns out that no significant quantities of cyanoacetylene are generated in any of the atmospheric models we consider.

Changes to the methanol chemistry (Tsai et al., 2017), are included, and not expected to make much difference here. The STAND2019 network, which appears first in this paper with new reaction numbers, is included in full in the Supplementary Information. The number of reactions is large (over 5000), but only a relatively small number of reactions are relevant for the HCN chemistry. The reactions relevant for atmospheric HCN production, by UV photons as well as by impacts, lighting and energetic particle interactions, are discussed in detail in Section 3. These reactions depend on the abundances of other species, which are determined by yet other reactions, and so we use the entire network when modeling the atmospheric photochemistry.

Finally, for the alterations in the stellar spectrum in Section 4.1, we take a model spectrum (Claire et al., 2012), and artificially enhance or reduce the spectrum within the regions of 500 Å- 1000 Å and 1000 Å- 2000 Å, as shown in Fig. 3, to test the impact of the UV spectrum on HCN formation.

3. Theory

In an exoplanet atmosphere composed of molecules bearing hydrogen, carbon, oxygen and nitrogen, there are two necessary conditions for producing HCN. First, the nitrogen bonds need to be cleaved, and then second, carbon needs to win over oxygen in the competition for the free nitrogen. The first condition can be relatively easy if the nitrogen is primarily in the form of ammonia (NH_3), which has a large absorption cross section over a wider wavelength range than N_2 ($\lesssim 300$ nm for ammonia compared to $\lesssim 160$ nm for N_2). Hot temperatures can also be sufficient to cleave a hydrogen atom from ammonia. Nitrogen in the form of N_2 , with a strong triple bond, is far more difficult to break apart. Impacts and lightning are sufficient to dissociate N_2 into $\text{N} + \text{N}$, as are UV photons of sufficiently short wavelength ($\lesssim 110$ nm), although these are largely attenuated below the thermosphere by N_2 itself, assuming that N_2 is a prevalent atmospheric constituent.

After the nitrogen bonds are broken, the nitrogen atoms react readily with nearby molecules, including some otherwise stable molecules. The simplest (and often the most common) case is if a lone nitrogen atom finds another lone nitrogen atom, in which case it will react to form N_2 . If there is a great deal of hydrogen available,

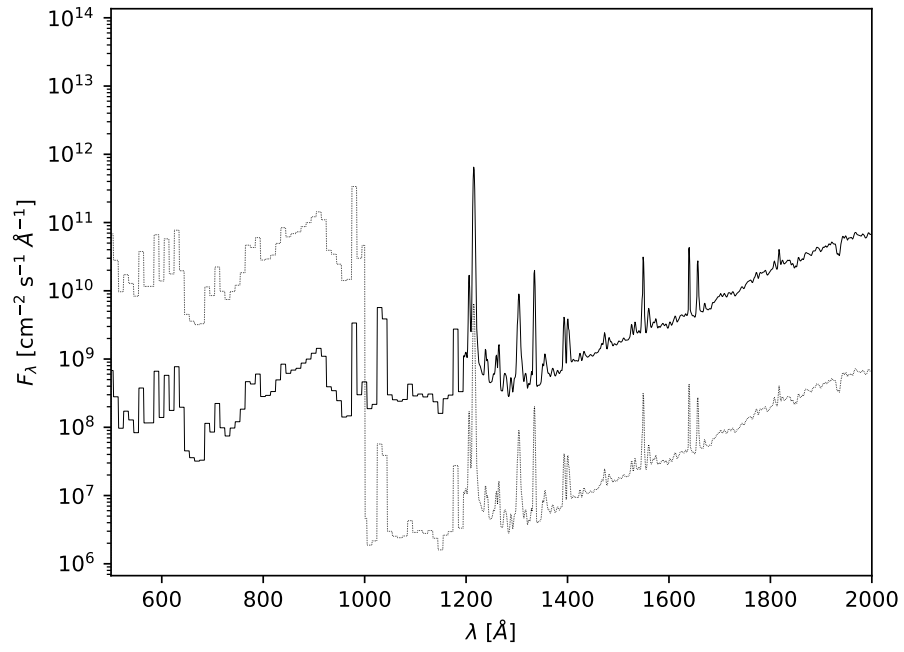


Figure 3: The spectrum of the young Sun (solid line) (Claire et al., 2012), artificially enhanced between 500 Å- 1000 Å and suppressed between 1000 Å- 2000 Å(dashed line), used to generate the results in Section 4.1.

whether in the form of H or H₂, the nitrogen will rapidly react to form NH or NH₂, and then will continue to react with the abundant hydrogen to end in ammonia. On the other hand, if the nitrogen atom collides with an oxygen atom, the resulting eventual product will generally be NO or NO₂. If the nitrogen atom finds carbon, the eventual product will generally be HCN. Thus the balance of carbon to oxygen in a given geological environment is a key metric to understanding abiotic nitrile chemistry. Fig's 4 and 5 provide the reaction networks for the formation and destruction of HCN under a variety of circumstances.

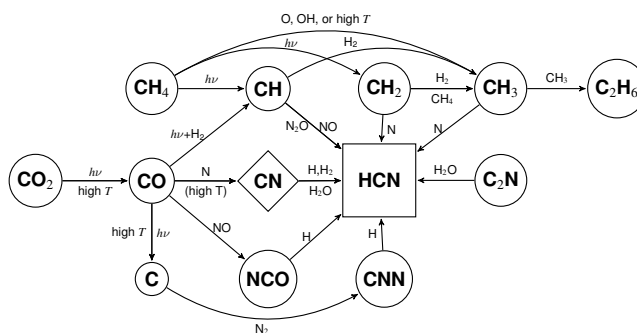


Figure 4: Collection of known pathways to form HCN on rocky planets. HCN can be produced photochemically (this paper, as well as Zahnle 1986 and Tian et al. 2011), by impacts (Ferus et al., 2017), and by lightning (Ardaseva et al., 2017). The rate constants for these reactions can be found in the STAND2019 Network (Supplementary Information).

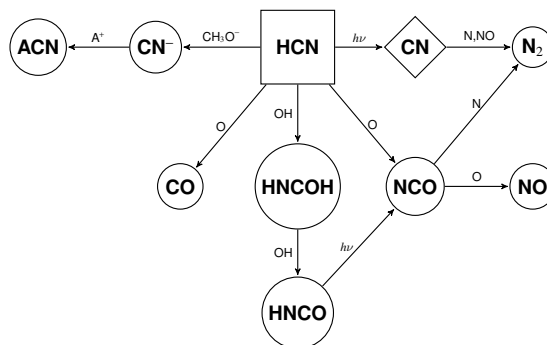


Figure 5: Collection of known pathways to destroy HCN on rocky planets. Destruction is primarily via atomic oxygen, the hydroxyl radical, anion chemistry, or photodissociation of HCN followed by reaction with atomic nitrogen or NO. The rate constants for these reactions can be found in the STAND2019 Network (Supplementary Information).

There are two ways to look at this competition: in terms of equilibrium and kinetics. Chameides & Walker were first to examine the thermochemical equilibrium of NO and HCN. They discuss the competition between carbon and oxygen for the nitrogen (Chameides and Walker, 1981), and express this competition in terms of the oxidation state of the carbon, where if the available carbon is mostly in the form of carbon

monoxide (CO) and methane (CH₄), more HCN will result, and if it is mostly in the form of CO₂, more NO will result. Chameides and Walker (1981) show this relation explicitly in terms of the C/O ratio in their Fig. 3.

We examine the thermochemical formation of HCN as a function of the C/O ratio, and find that we reproduce the results of Chameides and Walker (1981). Where C/O < 1 and the nitrogen bonds are broken, NO is formed in large quantities and HCN in trace quantities. If the C/O > 1 and the nitrogen bonds are cleaved, the opposite holds, and a great deal of HCN is formed with very little NO. If C/O \approx 1, then both HCN and NO are formed in reasonable quantities. These results match those of Chameides and Walker (1981, their Fig. 3). Methane is not necessary. All of the carbon could be in the form of CO or C₂H₂. What is necessary is an elemental C/O ratio \geq 1 and a reasonable amount of hydrogen, whether bound as methane, acetylene, molecular hydrogen, or even water vapor.

3.1. Mechanisms for Generating and Destroying HCN on Rocky Exoplanets

The mechanisms by which HCN is formed and destroyed vary with atmospheric composition, temperature, stellar activity, impact rate, surface processes, and lighting rates. The chemical mechanisms themselves do not change for each process, so it is helpful to look at the chemistry as a whole. Fig. 4 illustrates the pathways that can form HCN from CO₂, CO, C₂N (the most abundant CN-containing species produced by lightning on the Early Earth (Ardaseva et al., 2017)), as well as the formation from CH₄ (Zahnle, 1986; Tian et al., 2011; Airapetian et al., 2016). Some of the reactions are photochemical, denoted by $h\nu$, and require photons of a given range of wavelengths, and these may involve reactive intermediates, e.g. H₂CN, in the case of CH₂ + N. Other reactions are driven by energetic particles, and some proceed at high temperatures. These driving factors are rarely exclusive.

On some exoplanets, especially those with high C/O ratios, there may be a significant amount of carbon monoxide present in the atmosphere to begin with. For volcanically degassed atmospheres, the composition will largely depend on the outgassing pressure and redox state of the crust and upper mantle (Gaillard and Scaillet, 2014). Otherwise, CO is produced in reasonable quantities by the photodissociation or thermal dissociation of CO₂ (< 195 nm, $E_a \sim 415$ kJ/mol). At very high temperatures ($E_a = 300$ kJ/mol), CO + N \rightarrow CN + O, and once temperatures drop, the CN can proceed to HCN. CO itself can be dissociated (< 110 nm for CO(X¹ Σ^+), < 210 nm for CO(A³ Π), $E_a = 1000$ kJ/mol).

The destruction of HCN (see Fig. 5) proceeds on both the present and Early Earth primarily via oxidation by atomic oxygen and hydroxyl radicals (e.g. R7). In environments like Titan, with very high C/O ratios, where there is virtually no available oxygen, HCN is destroyed by photodissociation into CN followed by electron exchange from anions to form CN⁻.

HCN can also react with the hydroxyl radical and a third body in order to form HNCOH, a radical precursor to formamide, potentially relevant to prebiotic chemistry (Saladino et al., 2001; Ferus et al., 2015). Most often, though, HNCOH will encounter a second OH radical, forming isocyanic acid (HNCO). Isocyanic acid is quite susceptible to photodissociation, resulting in H + NCO.

Finally, HCN can become absorbed into water droplets, and there has the opportunity to react with a solvated electron, leading to the formation of formaldehyde, or its conjugate base can react with formaldehyde to form glycolonitrile. These are the initial steps toward RNA precursors (Ritson and Sutherland, 2012). The Henry’s Law constant for HCN is about 10 M/bar, and so resulting concentration of HCN in raindrops from the model atmosphere we present blow (C/O ratio of 0.55) is at most 10 nM, which is too small a concentration to be useful for prebiotic chemistry. If the atmospheric C/O ratio approaches 1, the surface mixing ratios could become as high as 10 ppm, and the resulting concentrations at 0.1 mM, on the cusp of prebiotically useful concentrations. The concentrations could be enhanced by overcoming Henry’s Law, e.g. by the absorption of formaldehyde (HCHO) by raindrops, and the reaction of formaldehyde with HCN in the droplet (Granville-Willett et al., 2018).

4. Results

We present our results for the HCN photochemistry as a function of the C/O ratio and UV flux (Section 4.1), and as a function of the barrier to destruction by atomic oxygen (Section 4.2).

4.1. The C/O Ratio, UV Flux and HCN Photochemistry

Regarding the C/O ratio, the photochemistry follows thermochemistry (Fig. 6). Given an atmosphere dominated by N_2 :

- **$C/O \leq 0.5$:** The production of HCN is low, with mixing ratios of < 1 ppm, regardless of the particular atmospheric composition.
- **$0.5 < C/O \leq 1.5$:** The production of HCN varies widely, with mixing ratios ranging from 1 ppm to 1000 ppm. In this regime, the particular atmospheric composition is important. If the atmosphere is 90% N_2 and 10% CO, HCN mixing ratios only come to 10 ppm, but if the atmosphere is 90% N_2 , 5% CO_2 and 5% CH_4 , the HCN mixing ratio reaches 500 ppm.
- **$C/O > 1.5$:** The production of HCN is high, with mixing ratios of > 0.1 % of the atmosphere, regardless of the particular atmospheric composition.

Photochemical production of HCN depends on the UV stellar spectrum. The EUV photons (which here we restrict to photons of wavelength $500 \text{ \AA} - 1000 \text{ \AA}$) dissociate the N_2 bond, and artificially enhancing the flux in this wavelength range (see Methods) leads to more HCN. The FUV (here between $1000 \text{ \AA} - 2000 \text{ \AA}$) flux tends to dissociate H_2O , producing free OH and O that readily destroy HCN (see Fig. 5). Artificially enhancing the flux in this wavelength range leads to less HCN. Fig. 7 shows the effect of artificially enhancing or reducing the spectrum in these wavelength ranges. This highlights the importance of the UV environment for the HCN abundance. Stars tend to have roughly 1:1 ratios of EUV and FUV light, and so deviations that would enhance or reduce HCN will mostly be due to atmospheric attenuation at specific wavelengths of light, or spectral variability due to stellar activity (e.g. flaring).

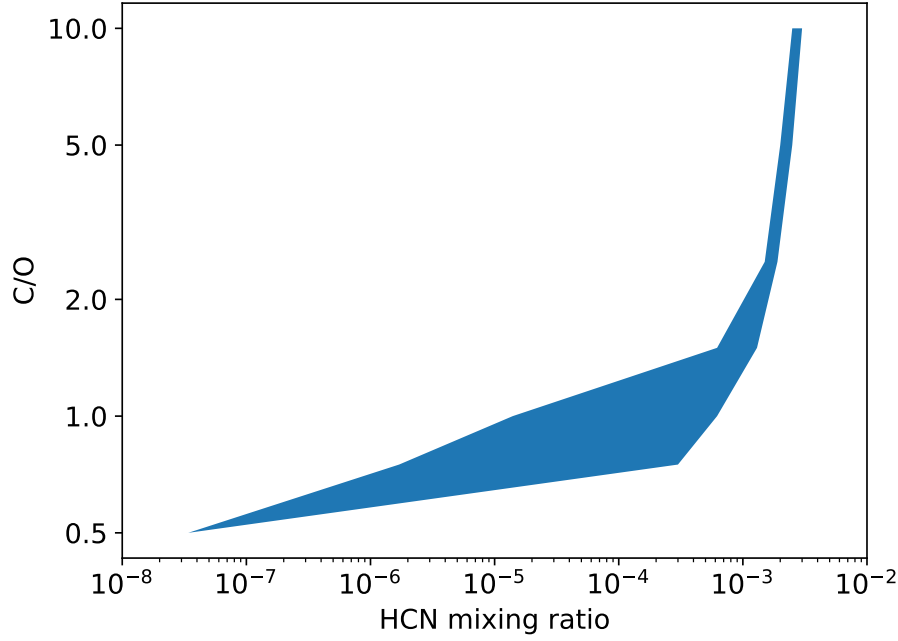


Figure 6: HCN mixing ratio as a function of the C/O ratio, applied to a 0.1 mbar gas composed of various ratios of CH₄, CO and CO₂, mixed with a 0.9 mbar gas composed of 99% N₂, 1% H₂O vapor and 0.1% H₂, exposed to the ultraviolet flux of the young Sun. The region spans several orders of magnitude, and the range can be explained by the variety of ways one can combine carbonaceous gases to achieve the same C/O ratio. For example, C/O=1 can be achieved by having a pure CO gas, or by having a gas of 50% CO₂ and 50% CH₄. The composition will depend on outgassing pressure and redox state (Gaillard and Scaillet, 2014). For a given C/O ratio, the presence of methane leads to considerably more HCN.

4.2. Atomic Oxygen as an HCN Sink and Atmospheric Methylamine

As with any molecule, the mixing ratio of HCN is determined by a balance of formation and loss. Hydroxyl radicals and atomic oxygen are the prime sinks of HCN. The rate constants for HCN destruction by O and OH are not all well-constrained. In particular, for the reaction:



There are several choices for the rate constant from the literature. The energy barriers, including error bars, range from ~ 20 kJ/mol (Louge and Hanson, 1985) to over 100 kJ/mol (Tsang and Herron, 1991), and values in between (Perry and Melius, 1985). We vary the rate constant of Reaction 7 for a model atmosphere of bulk composition 89% N₂, 10% CO₂ and 1% CH₄, one of the suite of atmospheres from Rugheimer & Rimmer (Rugheimer and Rimmer, 2018), following Rugheimer et al (Rugheimer and Kaltenegger, 2018). The temperature profile is determined using a climate model, and the photochemistry is calculated with this temperature profile and a young solar evolution model (see Methods and Fig. 2). The results for HCN and methylamine (CH₅N) are shown in Fig. 8.

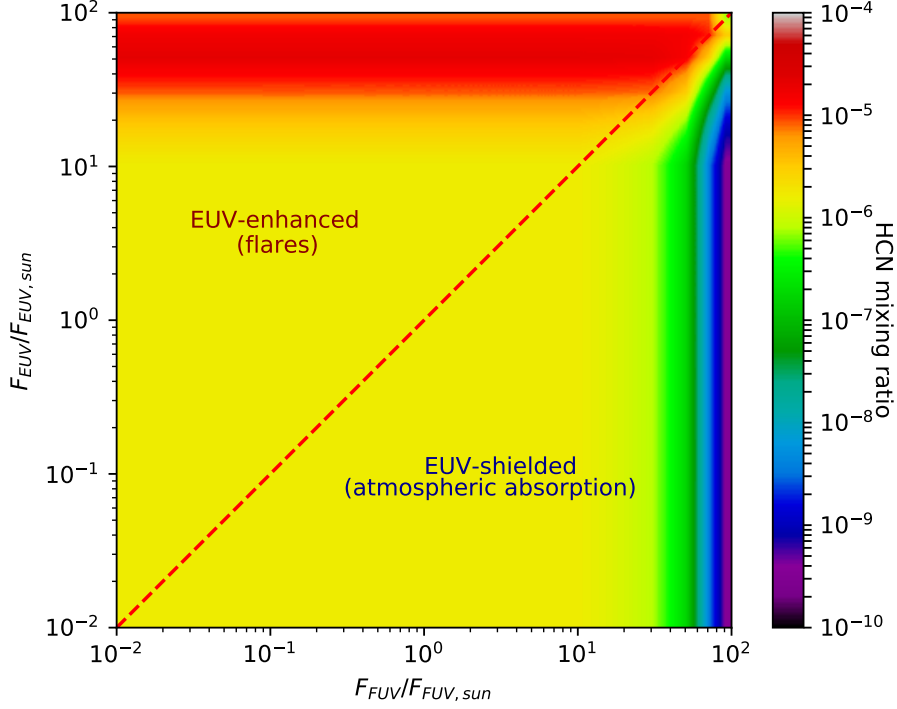
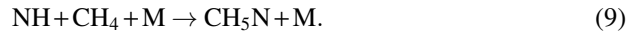
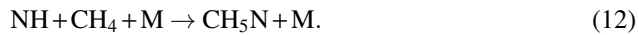
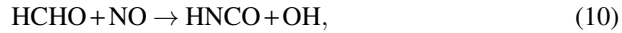


Figure 7: Ratio of a star’s UV spectral irradiance to solar spectral irradiance, $F_\lambda / F_{\lambda,\text{sun}}$ at EUV (500-1000 Å) and FUV (1000-2000 Å) wavelengths. 500-1500 Å light dissociates N_2 , the first step toward forming HCN photochemically. FUV photons dissociate H_2O , leading to hydroxyl radicals and free oxygen atoms, which rapidly destroy HCN. The dashed red line indicates where all main-sequence stellar quiescent emission lies. Stellar flares or atmospheric absorption may cause the spectrum to deviate from this line. Atmospheric absorption in particular will preferentially block the 500-1000 Å photons, pushing the photoexposed atmosphere into the bottom right region of the plot.

The amount of HCN in the atmosphere is clearly sensitive to the energetic barrier for R7. Surprisingly, the amount of methylamine in the upper atmosphere is enhanced as the energetic barrier for HCN destruction by atomic oxygen is lowered. This is because after HCN is destroyed, its products react as follows:



Near the surface ($p > 0.5$ bar), the amount of methylamine is only weakly dependent on the energy barrier for R7, because there is less atomic oxygen available to produce NCO. Methylamine is instead produced near the surface by:



To better assess the production of both HCN and methylamine on rocky exoplanets, the rate constants for $\text{HCN} + \text{O}$ in particular needs to be better constrained.

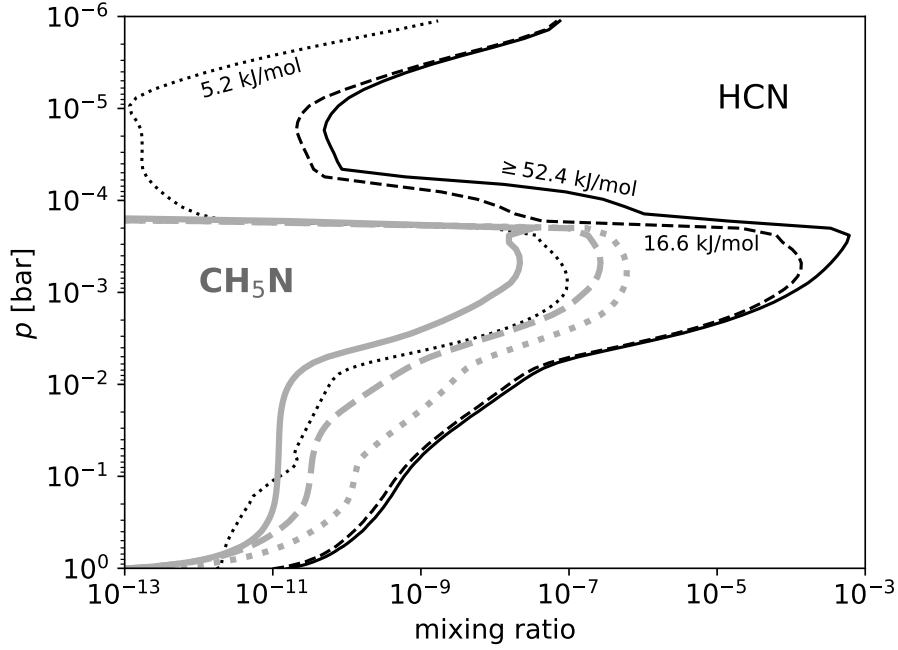


Figure 8: Mixing ratios of HCN (thin black) and methylamine (CH_5N , thick gray) as a function of pressure [bar], for a variety of energetic barriers for R7, ranging from 5.2 kJ/mol to 52.4 kJ/mol, with the most probable barrier lying between 16.6 and 52.4 kJ/mol, according to theory and experiment.

5. Discussion and Conclusions

We have shown that HCN abundances in the atmospheres of Earth-like rocky planets (N_2 dominated) depend critically on the atmospheric C/O ratio, with significantly greater amounts of HCN generated photochemically when $\text{C/O} \gtrsim 1$, regardless of the carbon-bearing species, whether it be CH_4 , CO , or C_2H_2 . In addition, the tropospheric HCN concentration is determined by the rate of HCN destruction by atomic oxygen. We explore the effect of adjusting the barrier for the reaction $\text{HCN} + \text{O} \rightarrow \text{NCO} + \text{H}$. The more efficient this reaction, the lower the tropospheric HCN concentrations, but the higher the concentrations of methylamine (CH_5N), a species that helps facilitate the prebiotic activation of nucleotides (Mariani et al., 2018).

When comparing our photochemistry results to alternative scenarios for forming HCN, such as impact delivery and production and production via lightning, these scenarios only require that the local C/O ratio be $\gtrsim 1$, and tend to produce HCN in greater quantities, 0.1-1% concentrations in the case of impacts and lightning shocks, versus 1-100 ppm tropospheric concentrations for the photochemical production of HCN. The

amount of HCN generated in impacts and lightning shocks is therefore more likely to achieve concentrations of HCN used in the lab. If the global C/O ratio is $\gtrsim 1$ within the atmosphere of a rocky exoplanet, this would suggest that prebiotic chemistry starting with HCN could be initiated in any surface environment for that planet, rather than in certain more exotic scenarios. Such environmental universality may be advantageous for originating life on the surfaces of planets with long-lived reducing atmospheres.

As shown above, the formation of HCN depends on the availability of nitrogen. All of our models have started with ~ 1 bar of nitrogen in the form of N_2 . The concentration of N_2 will be very difficult to detect remotely on an exoplanet, owing to the molecule's lack of a dipole moment. Airapetian et al. (2017) propose a novel observational strategy to constrain the N_2 content of exoplanet atmospheres by searching for photochemical products, especially NO. In more reduced atmospheres, NH_3 and HCN itself could be the major photochemical products of N_2 destruction. Either of these species would absorb at $1.5 \mu m$, appearing as a wing on the $1.4 \mu m$ water feature, as has been observed in the atmosphere of HD209458b (MacDonald and Madhusudhan, 2017). The shape and strength of these features will not be so strong in a temperate atmosphere with a significantly greater molecular weight. HCN will also have prominent broad features in the 7 and $14 \mu m$ regions, although at low resolution these will be difficult to disentangle from other species with similar spectra, such as C_2H_2 (Tessenyi et al., 2013). HCN could be distinguished from these other species at high resolution. Indeed, HCN has been detected in HD209458b in emission at high resolution (Hawker et al., 2018). The search for tracers of atmospheric conditions favorable to prebiotic chemistry is beyond the scope of this paper.

The C/O ratio has been seen as an important dimension for characterizing exoplanet atmospheres (Madhusudhan, 2012), and is clearly an important dimension when considering the production of hydrogen cyanide. It will likely be easier to constrain the C/O ratio for exoplanet systems in the near future than the nitrogen content, although both are essential for the photochemical production of HCN. The C/O ratio can be considered at a number of different scales, in order of decreasing size: cosmic, galactic, cluster, stellar, disk, sub-disk, planetary, surface and atmospheric C/O, and the C/O ratio within particular local environments. We will discuss each of these briefly in this order.

The cosmic C/O ratio increases over time, and within our galaxy, is expected to increase towards the galactic center, and to be enhanced in clusters with higher metallicity (Esteban et al., 2005). As low mass stars evolve and reach the asymptotic giant branch (AGB), carbon and other s-process elements are preferentially dredged up to the surface where they are released to the interstellar medium by the AGB winds (Wiescher et al., 2010). Therefore as the Universe ages, and increasingly more low mass stars evolve and die, the ratio of C/O will increase. Eventually, perhaps 30-50 Gyr from now, carbon will be more abundant than oxygen on average. This will drastically effect the geochemistry on planets produced from such an environment.

When the C/O ratio of a star exceeds 0.8, formation models suggest that planets can be produced in the disk with overall $C/O > 1$ (Bond et al., 2010). A small fraction of stars meet this criterion (Fortney, 2012), and so, even today, more carbon rich areas of the disk could form these so-called ‘‘Carbon Planets’’ (Kuchner and Seager, 2005). When the C/O ratio is < 0.8 , carbon-enhanced planets can still be formed near

the midplane of the disk, sufficiently far from the host star (Öberg et al., 2011), the distance being determined by ice lines and also by the formation mechanism (Booth et al., 2017).

Once a planet’s carbon is greater in abundance than oxygen by number, a few interesting chemical consequences will take place. First any oxygen will go into producing CO (Lodders and Fegley Jr, 1997). There will still be carbon left after the oxygen is depleted, and this will then bond with silicon, forming silicon carbide, SiC, titanium carbide, TiC, or will bind with itself to form graphite (Lodders and Fegley Jr, 1997). On Earth, the extra oxygen bonds with silicon forming silicates, the most abundant chemical species in Earth’s crust. SiC, however, is known to be an extremely durable mineral. Since carbon bonds are stronger than oxygen, it is more difficult to melt and break these bonds. Thus plate tectonics and weathering would be more difficult with silicon carbide rocks rather than silicates. Both of these effects may cause problems in maintaining a carbon cycle on such a planet and thus a long-term habitable climate.

For stars with a lower C/O ratio, like our Sun ($C/O \approx 0.55$ (Asplund et al., 2009)), formation in different parts of the disk will still affect the C/O ratio, but will probably not form “carbon planets”. But the story doesn’t end there. During and after planet formation, carbon is differentiated either into the core (carbon at high pressure becomes a siderophile (Dasgupta, 2013)), or into the crust and atmosphere, in the form of SiC (Dasgupta, 2013; Bond et al., 2010), graphite (Dasgupta, 2013; Frost and McCammon, 2008), or outgassed as CO_2 , CO, CH_4 (Gaillard and Scaillet, 2014), or C_2H_2 (Hu and Seager, 2014). At least one object in our Solar System, Titan, has an atmosphere and crust with a C/O ratio $\gg 1$ (Lunine and Atreya, 2008). There is evidence that more than 3.8 Ga, the Earth’s surface may also have had a C/O ratio $\gtrsim 1$ (Yang et al., 2014). Finally, it is worth noting that local C/O ratios vary by orders of magnitude even on the present-day Earth with its oxidized crust and atmosphere (Fischer, 2008), with mud volcanos releasing gas with ratios of $C/O \approx 100$ (Hedberg, 1974; Etiope and Milkov, 2004).

The debate about the C/O ratio continues (Sing et al., 2016; MacDonald and Madhusudhan, 2017), and hopefully the advent of JWST will be able to provide some clarity on this question. The persistent connection between the production of HCN and the C/O ratio implies that there is a connection between a rocky planet’s C/O ratio and the chances for life to originate on its surface via any chemical pathway involving HCN. This C/O ratio, along with a better understanding of stellar UV spectra (Ranjan and Sasselov, 2016, 2017; Rimmer et al., 2018) and nitrogen content of exoplanets (Airapetian et al., 2016; Airapetian et al., 2017) may be key for determining whether a given rocky planet lies within the abiogenesis zone.

Acknowledgements

P. B. R. acknowledges support by the Simons and Kavli Foundations for this work, including Simons Foundation SCOL awards 599634. S. R. acknowledges support by a grant from the Simons Foundation (SCOL awards 339489). This work has made use of the MUSCLES M dwarf UV radiation field database. P. B. R. thanks Sukrit Ranjan and Dimitar Sasselov for helpful comments.

References

- Airapetian, V. S., Glocer, A., Gronoff, G., Hebrard, E., Danchi, W., 06 2016. Prebiotic chemistry and atmospheric warming of early earth by an active young sun. *Nature Geosci* 9 (6), 452–455.
- Airapetian, V. S., Jackman, C. H., Mlynczak, M., Danchi, W., Hunt, L., Nov. 2017. Atmospheric Beacons of Life from Exoplanets Around G and K Stars. *Scientific Reports* 7, 14141.
- Ardayeva, A., Rimmer, P. B., Waldmann, I., Rocchetto, M., Yurchenko, S. N., Helling, C., Tennyson, J., Apr. 2017. Lightning Chemistry on Earth-like Exoplanets. *ArXiv e-prints*.
- Asplund, M., Grevesse, N., Sauval, A. J., Scott, P., Sep. 2009. The Chemical Composition of the Sun. *ARAA*47, 481–522.
- Becker, R. S., Hong, J., 1983. Photochemistry of acetylene, hydrogen cyanide, and mixtures. *The Journal of Physical Chemistry* 87 (1), 163–166.
- Bond, J. C., O’Brien, D. P., Lauretta, D. S., Jun. 2010. The Compositional Diversity of Extrasolar Terrestrial Planets. I. In Situ Simulations. *ApJ*715, 1050–1070.
- Booth, R. A., Clarke, C. J., Madhusudhan, N., Ilee, J. D., Aug. 2017. Chemical enrichment of giant planets and discs due to pebble drift. *MNRAS*469, 3994–4011.
- Chameides, W. L., Walker, J. C. G., Dec. 1981. Rates of Fixation by Lightning of Carbon and Nitrogen in Possible Primitive Atmospheres. *Origins of Life* 11, 291–302.
- Claire, M. W., Sheets, J., Cohen, M., Ribas, I., Meadows, V. S., Catling, D. C., Sep. 2012. The Evolution of Solar Flux from 0.1 nm to 160 μ m: Quantitative Estimates for Planetary Studies. *ApJ*757, 95.
- Dasgupta, R., Jan. 2013. Ingassing, Storage, and Outgassing of Terrestrial Carbon through Geologic Time. *Reviews in Mineralogy and Geochemistry* 75, 183–229.
- Esteban, C., García-Rojas, J., Peimbert, M., Peimbert, A., Ruiz, M. T., Rodríguez, M., Carigi, L., Jan. 2005. Carbon and Oxygen Galactic Gradients: Observational Values from H II Region Recombination Lines. *ApJL*618, L95–L98.
- Etioppe, G., Milkov, A. V., 2004. A new estimate of global methane flux from onshore and shallow submarine mud volcanoes to the atmosphere. *Environmental Geology* 46 (8), 997–1002.
- Ferris, J. P., Orgel, L. E., 1966. An unusual photochemical rearrangement in the synthesis of adenine from hydrogen cyanide. *Journal of the American Chemical Society* 88 (5), 1074–1074.

- Ferus, M., Kubelík, P., Knížek, A., Pastorek, A., Sutherland, J., Civiš, S., 2017. High energy radical chemistry formation of hcn-rich atmospheres on early earth. *Scientific reports* 7 (1), 6275.
- Ferus, M., Nesvorný, D., Šponer, J., Kubelík, P., Michalčíková, R., Shestivská, V., Šponer, J. E., Civiš, S., Jan. 2015. High-energy chemistry of formamide: A unified mechanism of nucleobase formation. *Proceedings of the National Academy of Science* 112, 657–662.
- Fischer, T. P., 2008. Fluxes of volatiles (h₂o, co₂, n₂, cl, f) from arc volcanoes. *Geochemical Journal* 42 (1), 21–38.
- Fortney, J. J., Mar. 2012. On the Carbon-to-oxygen Ratio Measurement in nearby Sun-like Stars: Implications for Planet Formation and the Determination of Stellar Abundances. *ApJL* 747, L27.
- Frost, D. J., McCammon, C. A., May 2008. The Redox State of Earth's Mantle. *Annual Review of Earth and Planetary Sciences* 36, 389–420.
- Gaillard, F., Scaillet, B., Oct. 2014. A theoretical framework for volcanic degassing chemistry in a comparative planetology perspective and implications for planetary atmospheres. *Earth and Planetary Science Letters* 403, 307–316.
- Gao, P., Hu, R., Robinson, T. D., Li, C., Yung, Y. L., Jun. 2015. Stability of CO₂ Atmospheres on Desiccated M Dwarf Exoplanets. *ApJ* 806, 249.
- Granville-Willett, A., Archibald, A. T., Rimmer, P. B., Griffiths, P., Sutherland, J. D., 2018. Overcoming Henry's Law. in prep.
- Haqq-Misra, J. D., Domagal-Goldman, S. D., Kasting, P. J., Kasting, J. F., 2008. A revised, hazy methane greenhouse for the archaean earth. *Astrobiology* 8 (6), 1127–1137.
- Hawker, G. A., Madhusudhan, N., Cabot, S. H. C., Gandhi, S., Aug. 2018. Evidence for Multiple Molecular Species in the Hot Jupiter HD 209458b. *ApJL* 863, L11.
- Hedberg, H. D., 1974. Relation of methane generation to undercompacted shales, shale diapirs, and mud volcanoes. *AAPG Bulletin* 58 (4), 661–673.
- Hu, R., Seager, S., Mar. 2014. Photochemistry in Terrestrial Exoplanet Atmospheres. III. Photochemistry and Thermochemistry in Thick Atmospheres on Super Earths and Mini Neptunes. *ApJ* 784, 63.
- Kharecha, P., Kasting, J. F., Siefert, J., 2005. A coupled atmosphere–ecosystem model of the early archaean earth. *Geobiology* 3, 53–73.
- Kuchner, M. J., Seager, S., Apr. 2005. Extrasolar Carbon Planets. *ArXiv Astrophysics e-prints*.

- Lodders, K., Fegley Jr, B., 1997. In astrophysical implications of the laboratory study of presolar materials; bernatowicz, tj; zinner, e., eds. In: AIP Conference Proceedings. Vol. 402. p. 391.
- Louge, M. Y., Hanson, R. K., 1985. Shock tube study of nco kinetics. In: Symposium (International) on Combustion. Vol. 20. Elsevier, pp. 665–672.
- Lunine, J. I., Atreya, S. K., Mar. 2008. The methane cycle on Titan. *Nature Geoscience* 1, 159–164.
- MacDonald, R. J., Madhusudhan, N., Aug. 2017. HD 209458b in new light: evidence of nitrogen chemistry, patchy clouds and sub-solar water. *MNRAS* 469, 1979–1996.
- Madhusudhan, N., Oct. 2012. C/O Ratio as a Dimension for Characterizing Exoplanetary Atmospheres. *ApJ* 758, 36.
- Mariani, A., Russell, D. A., Javelle, T., Sutherland, J. D., 2018. A light-releasable potentially prebiotic nucleotide activating agent. *Journal of the American Chemical Society* 140 (28), 8657–8661.
- Miller, S. L., 1957. The mechanism of synthesis of amino acids by electric discharges. *Biochimica et Biophysica Acta* 23, 480–489.
- Öberg, K. I., Murray-Clay, R., Bergin, E. A., Dec. 2011. The Effects of Snowlines on C/O in Planetary Atmospheres. *ApJL* 743, L16.
- Patel, B. H., Percivalle, C., Ritson, D. J., Duffy, C. D., Sutherland, J. D., Apr. 2015. Common origins of RNA, protein and lipid precursors in a cyanosulfidic protometabolism. *Nature Chemistry* 7, 301–307.
- Pavlov, A. A., Kasting, J. F., Brown, L. L., Rages, K. A., Freedman, R., 2000. Greenhouse warming by ch₄ in the atmosphere of early earth. *Journal of Geophysical Research: Planets* 105 (E5), 11981–11990.
- Perry, R. A., Melius, C. F., 1985. The rate and mechanism of the reaction of hcn with oxygen atoms over the temperature range 540–900 k. In: Symposium (International) on Combustion. Vol. 20. Elsevier, pp. 639–646.
- Pierrehumbert, R., Gaidos, E., Jun. 2011. Hydrogen Greenhouse Planets Beyond the Habitable Zone. *ApJL* 734, L13.
- Ranjan, S., Sasselov, D. D., Jan. 2016. Influence of the UV Environment on the Synthesis of Prebiotic Molecules. *Astrobiology* 16, 68–88.
- Ranjan, S., Sasselov, D. D., Mar. 2017. Constraints on the Early Terrestrial Surface UV Environment Relevant to Prebiotic Chemistry. *Astrobiology* 17, 169–204.
- Rimmer, P. B., Helling, C., May 2016. A Chemical Kinetics Network for Lightning and Life in Planetary Atmospheres. *The Astrophysical Journal Supplement Series* 224, 9.

- Rimmer, P. B., Xu, J., Thompson, S. J., Gillen, E., Sutherland, J. D., Queloz, D., 2018. The origin of rna precursors on exoplanets. *Science Advances* 4 (8), eaar3302.
- Ritson, D., Sutherland, J. D., 2012. Prebiotic synthesis of simple sugars by photoredox systems chemistry. *Nature chemistry* 4 (11), 895.
- Rugheimer, S., Kaltenegger, L., Feb. 2018. Spectra of Earth-like Planets through Geological Evolution around FGKM Stars. *ApJ* 854, 19.
- Rugheimer, S., Rimmer, P. B., 2018. Exoplanet Prebiosignatures. in prep.
- Saladino, R., Crestini, C., Costanzo, G., Negri, R., Di Mauro, E., 2001. A possible prebiotic synthesis of purine, adenine, cytosine, and 4 (3h)-pyrimidinone from formamide: implications for the origin of life. *Bioorganic & medicinal chemistry* 9 (5), 1249–1253.
- Sanchez, R. A., Ferbis, J. P., Orgel, L. E., 1967. Studies in prebiotic synthesis: II. synthesis of purine precursors and amino acids from aqueous hydrogen cyanide. *Journal of molecular biology* 30 (2), 223–253.
- Sanchez, R. A., Ferris, J. P., Orgel, L. E., 1966. Cyanoacetylene in prebiotic synthesis. *Science* 154 (3750), 784–785.
- Sanchez, R. A., Orgel, L. E., 1970. Studies in prebiotic synthesis: V. synthesis and photoanomerization of pyrimidine nucleosides. *Journal of molecular biology* 47 (3), 531–543.
- Sing, D. K., Fortney, J. J., Nikolov, N., Wakeford, H. R., Kataria, T., Evans, T. M., Aigrain, S., Ballester, G. E., Burrows, A. S., Deming, D., Désert, J.-M., Gibson, N. P., Henry, G. W., Huitson, C. M., Knutson, H. A., Lecavelier Des Etangs, A., Pont, F., Showman, A. P., Vidal-Madjar, A., Williamson, M. H., Wilson, P. A., Jan. 2016. A continuum from clear to cloudy hot-Jupiter exoplanets without primordial water depletion. *Nature* 529, 59–62.
- Strecker, A., 1854. Ueber einen neuen aus aldehyd-ammoniak und blausäure entstehenden körper. *Justus Liebigs Annalen der Chemie* 91 (3), 349–351.
- Tessenyi, M., Tinetti, G., Savini, G., Pascale, E., Sep. 2013. Molecular Detectability in Exoplanetary Emission Spectra. *European Planetary Science Congress* 8, EPSC2013–817.
- Tian, F., Kasting, J. F., Zahnle, K., Aug. 2011. Revisiting HCN formation in Earth's early atmosphere. *Earth and Planetary Science Letters* 308, 417–423.
- Toon, O. B., McKay, C. P., Ackerman, T. P., Santhanam, K., Nov. 1989. Rapid calculation of radiative heating rates and photodissociation rates in inhomogeneous multiple scattering atmospheres. *Journal of Geophysical Research: Atmospheres* 94, 16287–16301.

- Tsai, S.-M., Lyons, J. R., Grosheintz, L., Rimmer, P. B., Kitzmann, D., Heng, K., Feb. 2017. VULCAN: An Open-source, Validated Chemical Kinetics Python Code for Exoplanetary Atmospheres. *ApJS*228, 20.
- Tsang, W., Herron, J. T., 1991. Chemical kinetic data base for propellant combustion i. reactions involving no, no2, hno, hno2, hcn and n2o. *Journal of physical and chemical reference data* 20 (4), 609–663.
- Wiescher, M., Görres, J., Überseder, E., Imbriani, G., Pignatari, M., Nov. 2010. The Cold and Hot CNO Cycles. *Annual Review of Nuclear and Particle Science* 60, 381–404.
- Wordsworth, R., Pierrehumbert, R., Apr. 2014. Abiotic Oxygen-dominated Atmospheres on Terrestrial Habitable Zone Planets. *ApJL*785, L20.
- Xu, J., Ritson, D. J., Ranjan, S., Todd, Z. R., Sassellov, D. D., Sutherland, J. D., 2018. Photochemical reductive homologation of hydrogen cyanide using sulfite and ferrocyanide. *Chemical Communications* 54 (44), 5566–5569.
- Yang, X., Gaillard, F., Scaillet, B., May 2014. A relatively reduced Hadean continental crust and implications for the early atmosphere and crustal rheology. *Earth and Planetary Science Letters* 393, 210–219.
- Zahnle, K. J., Feb. 1986. Photochemistry of methane and the formation of hydrocyanic acid (HCN) in the Earth’s early atmosphere. *JGR*91, 2819–2834.